Rock Mech. Rock Engng. (2007) 40 (6), 563–576
DOI 10.1007/s00603-006-0122-7
Printed in The Netherlands

Rock Mechanics and Rock Engineering

Safety Management Based on Detection of Possible Rock Bursts by AE Monitoring during Tunnel Excavation

By

A. Hirata[1], **Y. Kameoka**[2], and **T. Hirano**[3]

[1] Department of Civil Engineering, Sojo University, Kumamoto, Japan
[2] Japan Construction Method and Machinery Research Institute, Fuji, Japan
[3] Nishimatsu Construction Co. Ltd., Tokyo, Japan

Received May 23, 2005; accepted August 23, 2006
Published online January 16, 2007

Summary

As underground development continues at great depths, the danger of rock bursts will inevitably increase. It is important to consider countermeasures for avoiding rock bursts in underground work. In Japan, rock bursts have actually been experienced during construction of several tunnels, including the Kan-etsu tunnel construction project, during which many rock bursts were observed. Stress analysis of tunnels is performed based on initial stress measurements in the base rock. In addition, AE measurement has been adopted in construction management, allowing safer excavation. Collective analysis of the data obtained has been shown to be effective for safety control during excavation of hard base rock. In this research, initial stress measurements in base rock, secondary stress analysis around a tunnel, and AE measurements are examined. Based on the results of this analysis, it is clear that the generation of rock bursts is related to the presence of geological discontinuities.

Keywords: Rock burst, safety management, AE monitoring, initial stress measurement.

1. Introduction

Rock burst is a phenomenon in which a mass of rock collapses explosively. In Japan, as the depths of coal and metal mines increased in order to keep pace with the demands of economic growth, incidents of ''rock noise'' and rock bursts became increasingly common (Iwasaki et al., 1972). Serious disasters resulting from rock bursts were especially common from the 1960s to the 1980s.

Around the same time, deep and lengthy tunneling of road and rail tunnels was conducted in order to coordinate with mining activities, resulting in reports of similar rock bursts. In particular, rock bursts were experienced during the excavation of three

railroad tunnels, the Shimizu tunnel (completed in 1931), the Shin-Shimizu tunnel (1967), and the Oh-Shimizu tunnel (1980), which were excavated directly under Mount Tanigawa-dake, at the border of Niigata Prefecture and Gumma Prefecture (Minemoto, 1968).

In the Kan-etsu tunnel construction project, 11 km of tunnels (two road tunnels and an evacuation tunnel) were built from 1977 to 1990 in the same area as the three railroad tunnels mentioned above, resulting in the natural generation of rock bursts (Nakamichi, 1975). As a result, rock stress measurements (Mitani et al., 1984) and AE measurements (Nakajima and Watanabe, 1984) were conducted, and the mechanism of rock bursts was quantitatively studied. Since rock bursts were also expected in the last phase of Kan-etsu tunnel construction, preparations were made for rock bursts before the excavation started, and investigation and analysis were performed through the working period (Hirata et al., 1991). In this study, the rock stress around the tunnel is discussed based on the initial stress measurements obtained in the rock burst field, and safety control based on AE monitoring is explained.

2. A District Famous for Rock Bursts

2.1 Rock Burst below Mt. Tanigawa-dake

The Kan-Etsu tunnel is located below Mt. Tanigawa-dake in the middle of Japan. Three railroad tunnels, the Shimizu tunnel (completed in 1931), the Shin-Shimizu tunnel (1967) and the Oh-Shimizu tunnel (1980), are located in the same district. Rock bursts occurred during the construction of every tunnel in the district, with the result that this area is famous in Japan for generating rock bursts. The Kan-etsu highway road project has two main tunnels and an evacuation tunnel. The evacuation tunnel and one of the main tunnels were first constructed between 1977 and 1985, and the second main tunnel was built from 1986 to 1990.

In the area where the rock bursts occurred, the overburden depth is between 230 m and 1000 m. Figure 1 is a longitudinal section of the tunnel. In the phase of construction shown in the diagram, excavation is taking place from the Yuzawa side to the

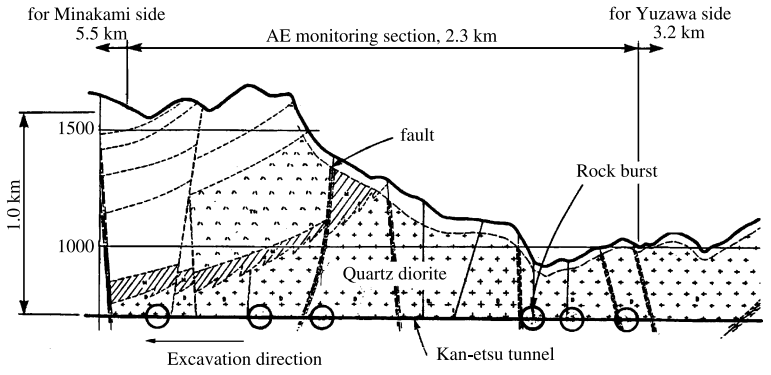

Fig. 1. Geological conditions and overburden in the Kan-etsu tunnel. Open circles represent rock burst sites

Minakami side. Circles show the rock burst sites. Most of the rock bursts occurred at the face after blasting, which is characteristic of rock bursts in areas with a shallow overburden, and none occurred at the sidewalls. However, it was reported that during construction of the three previously existing railroad tunnels, the number of rock bursts generated in the sidewalls was remarkable. Although rock bolts were installed, the rock bolts were left behind and the rock near the face was destroyed. Even when the rock did not break, cracks occurred on the sprayed concrete surface.

2.2 Geological Conditions and Tunnel Direction

In the Kan-etsu tunnel, rock bursts were generated only in areas where rock is quartz diorite. The uniaxial compressive strength of the rock was approximately 200 MPa. The rock at the face was fresh and there was no seepage of water from the wall of the tunnel; geological discontinuities were tightly closed. Figure 2 shows a plan of a rock burst hazard zone before excavation of a dust collection chamber. The hazard zone is not continuous, but occurs at intervals. No rock bursts occurred in this domain, but high rock noise was frequently noted. The major discontinuities intersecting the tunnels are shown by the short solid lines.

The distribution of geological discontinuities is shown in Fig. 3, as poles on a stereographic projection. Arrows indicate the direction of tunnel excavation. The direction of the Kan-etsu tunnel is 35° south of the Shimizu and Shin-Shimizu tunnels. Numerals in this figure are discontinuity numbers. A major group of discontinuities, surrounded by a dashed line in the diagram, intersects the direction of tunnel excavation. The dip angles of most discontinuities in the Kan-etsu tunnel range from 60 to 90°, and are relatively steep. The tunnel direction intersects the major group of discontinuities at an angle of 40–50°, and another set of discontinuities are conjugate to the first. The Shimizu tunnel and the Shin-Shimizu tunnel are located at greater depth than the Kan-etsu tunnel. The Oh-Shimizu tunnel intersects at the center of the angle made by the Shimizu and Shin-Shimizu tunnels. In the Shimizu

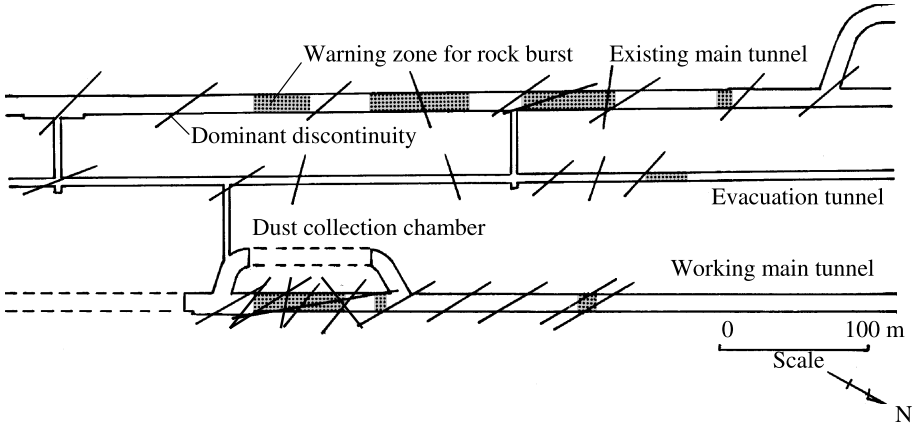

Fig. 2. Plan metric map of Kan-etsu tunnel

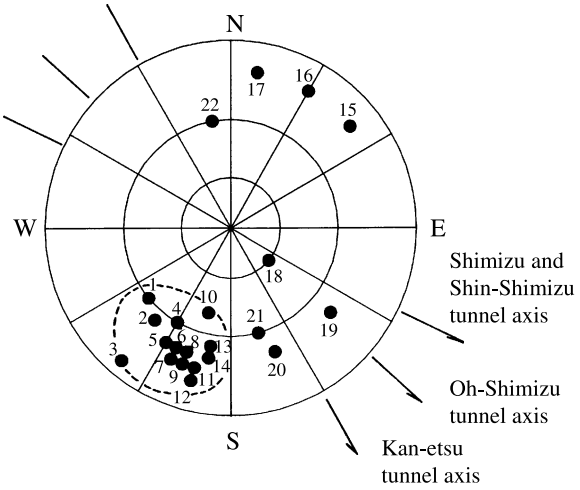

Fig. 3. Poles of major discontinuities surrounding rock burst site

and Shin-Shimizu tunnels, the major discontinuities appear along the direction of the tunnel axes.

2.3 Initial Rock Stress and Secondary Stress on Discontinuities

Three-dimensional initial stress measurement was carried out using an in situ stress measurement technique, a type of stress-release method called the hemispherical-ended borehole technique (Sugawara et al., 1985). This measuring method is based on the deformation of a hemispherical-ended borehole caused by stress release during over-coring. A strain gauge with 16 foils is pasted on the hemispherical borehole bottom and the three-dimensional stress state is elastically determined.

The measurement site, at a distance of 4682.7 m from the Yuzawa-side tunnel entrance, is shown in Fig. 4 as a plan view. Measurements were performed prior to excavation of the dust collection chamber. The overburden at the site is 820 m. Measurements were repeated at 8 points at distances ranging from 4.6 to 14.5 m from the tunnel wall, as shown in Fig. 5.

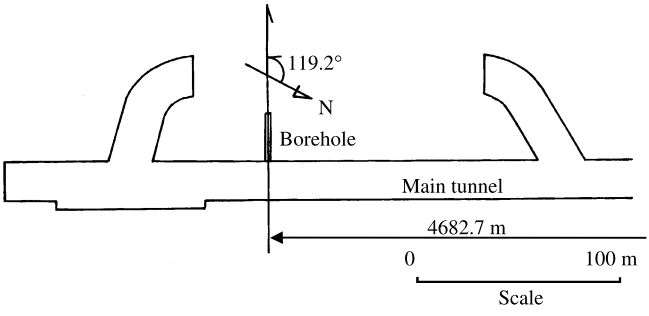

Fig. 4. Site at which initial rock stress was measured

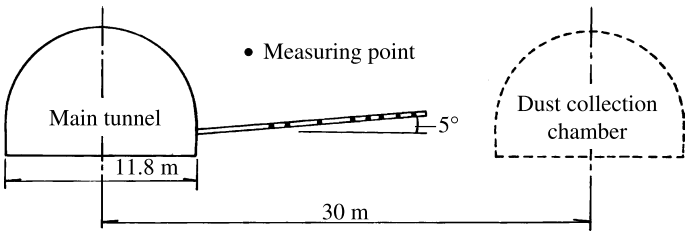

Fig. 5. Borehole and measuring points used in hemispherical-ended stress measurement method

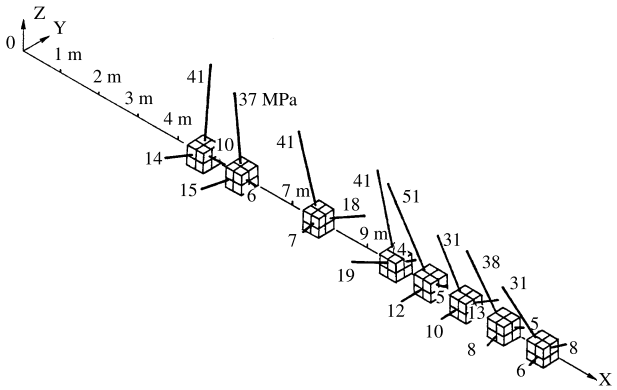

Fig. 6. Principal stresses along the measurement borehole

The distribution of the principal stresses along the borehole axis is shown in Fig. 6. The origin of the coordinates coincides with the wall of the tunnel. For a distance of up to 6 m from the tunnel wall, the rock stress is affected to a considerable extent by

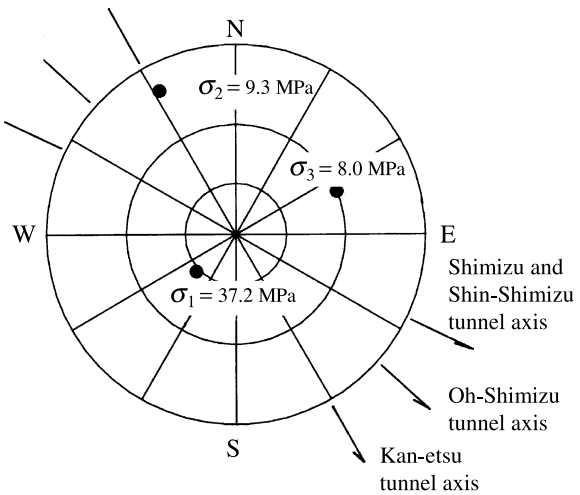

Fig. 7. Initial principal stresses shown on a stereographic projection map

the excavation of the tunnel, so that the maximum principal stress near the tunnel wall acts almost vertically. Similar stresses are observed up to 10 m from the wall. Thereafter, the initial rock stress is determined by using strain data measured at four points located at a distance from the tunnel wall greater than 10 m.

The initial principal stresses are plotted in Fig. 7, which is a lower-hemisphere stereographic projection. The maximum principal stress is 37.2 MPa, the intermediate principal stress is 9.3 MPa, and the minimum principal stress is 8.0 MPa. The magnitudes of the intermediate principal stress and the minimum principal stress are one-fourth and one-fifth, respectively, of the maximum principal stress. Furthermore, the intermediate principal stress is nearly parallel to the Kan-etsu tunnel axis. Thus, the maximum and minimum principal stresses act on the tunnel face, assuming that there is no change in the direction of the principal stresses around the tunnel. However, such a condition cannot be found in tunnels with other directions.

There is a characteristic discontinuity group in the base rock in which the tunnel is excavated. Figure 8 shows the relationship between the shear stress τ_n and the normal stress σ_n acting on the discontinuities, which are numbered as in Fig. 3. The solid circles represent the stresses acting on the discontinuities, as calculated from the initial rock stress, whereas the open circles represent stresses on the tunnel face. The straight lines connecting the two points represent the change from initial stress state to secondary stress state at the tunnel face.

In the calculation of the stresses at the tunnel face, it is assumed that the maximum principal stress and the minimum principal stress are equal to the initial stresses, and the intermediate principal stress is zero. The assumption is considered to be permissible, because the intermediate principal stress is almost normal to the tunnel face. The discontinuities No. 17, 19, 20 and 22 become easy to cause shear failure due to the excavation of the tunnel, whereas the dominant discontinuity is stable. However, taking into account the reports that sidewall rock bursts occurred frequently during construction of the other tunnels located below Mt. Tanigawa-dake, there is a considerable possibility that the dominant discontinuity may become unstable.

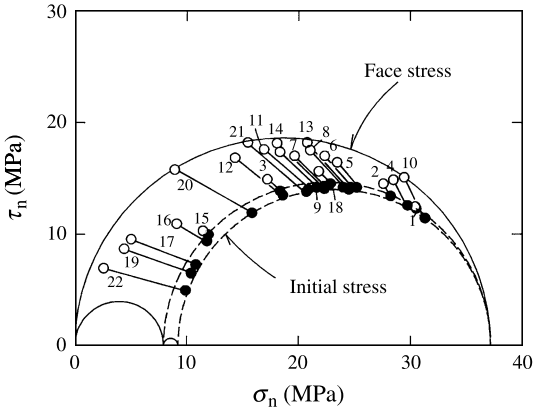

Fig. 8. Change from initial stress to face stress for the major discontinuities. Numerals represent the discontinuity number as shown in Fig. 3

Concentration of stress in the rock near the tunnel wall is necessary for the occurrence of rock bursts. However, if plastic deformation develops, brittle failures such as rock bursts do not occur. There is also no danger of rock burst if the rock strength is sufficient to offset the induced stress caused by excavation. Therefore, in order for a rock burst to occur, the strength of the rock mass must be moderate, and the existence of discontinuities of a particular strike and dip angle is required.

3. AE Monitoring and Excavation Management

3.1 AE Monitoring System

Acoustic emission monitoring was carried out in the Kan-etsu tunnels. In particular, during excavation of the main tunnel, it was carried out every day as a measure of safety management. Figure 9 shows the equipment used for measurement and safety management arranged in the evacuation tunnel. Four accelerometers with a resonance of 15 kHz were inserted into the rock of the evacuation tunnel to a depth of 1 m. The sensors were placed on top of the anchor bolts mortared at the bottom of boreholes

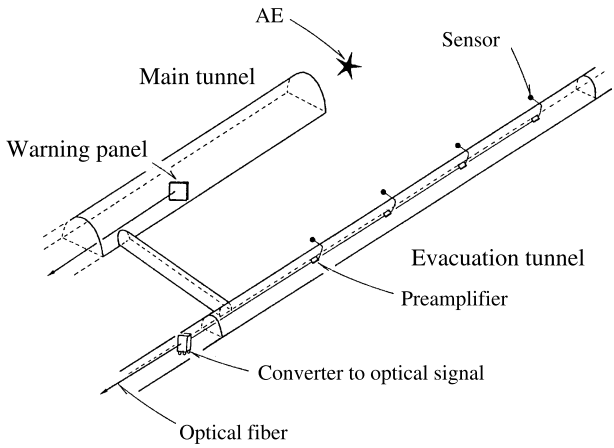

Fig. 9. Layout of equipment for AE monitoring

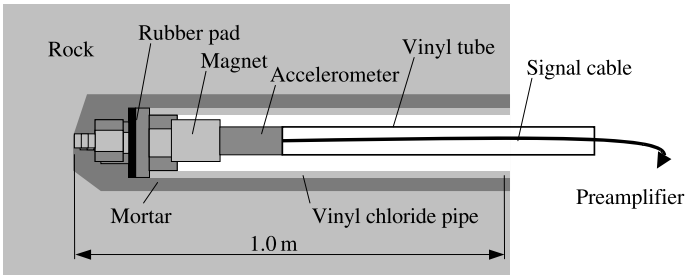

Fig. 10. Sensor placing technique

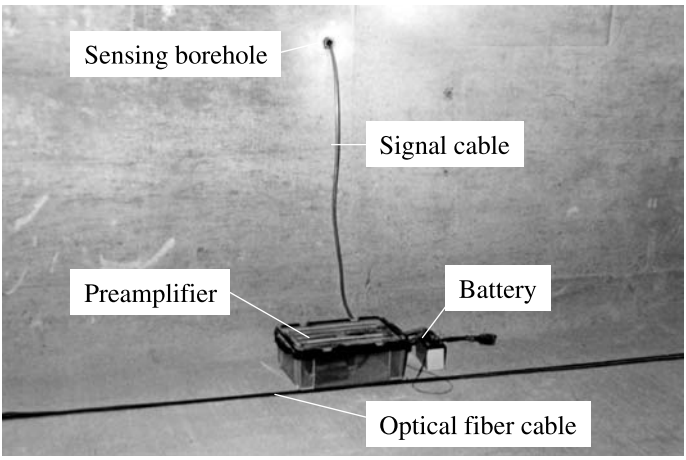

Fig. 11. Sensor is installed at the bottom of the borehole

using a magnet, as shown in Fig. 10. Figure 11 illustrates sensor installation on the wall of the evacuation tunnel. By adaptation of the installation method, noise from the evacuation tunnel side, such as wind and traffic noise, was prevented. The sensors were placed 20–24 m apart. The distance between the main tunnel face and the sensors was 70 and 100 m. The overall frequency characteristics of all instruments were nearly flat over a range of 100 to 5 kHz.

The signals observed by the sensor are amplified to 20 dB using a preamplifier and are then transmitted to an amplifier situated on a movable cart via a signal cable. Figure 12 shows the equipment used: the cart holds an amplifier, an AD converter, an optical signal converter, and a drum of optical fiber cable. It is converted into an optical signal, which is transmitted to a measurement office at a distance of 5–7 km.

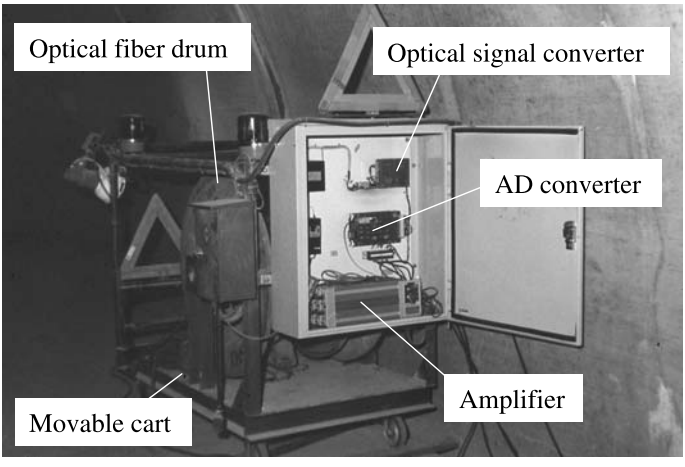

Fig. 12. Amplifier, optical fiber drum and optical signal converter on a movable cart in the evacuation tunnel

Fig. 13. Rock burst warning signal in the main tunnel during excavation

The AE waveform, the number of AE events, and a ring-down count are recorded on a hard disk as digitized data.

The sensor at the tail end moves to the forefront as the excavation of the main tunnel advances. As the cart moves, the fiber-optic cable is unwound from the drum. A warning signal, as shown in Fig. 13, is automatically switched on when 10 or more AE events are detected in 1 hour. The caution level at which a warning signal is sent was determined based on AE signals caused by rock bursts (Yamamoto and Taga, 1990).

3.2 Measured Waveforms and Source Location

AE monitoring was carried out when workers were close to the face, except during blasting. All AE waveforms were recorded on a hard disk. Examples of AE waveforms measured are shown in Fig. 14: six similar waveforms among those obtained during 8 hours of continuous measurement are arranged in order of measurement. Each waveform was measured at an arbitrary time during the 8 hours. Although the amplitudes are not the same, the waveforms are very similar. Two unique phases may be recognized. The first is the arrival of a P-wave, and the subsequent large-amplitude phase corresponds to the S-wave. The arrival of the P-wave and that of the S-wave show a time lag of $\Delta t = 16$ milliseconds. The straight-line distance between the sensor that measured these waveforms and the center of the tunnel face was 95.8 m.

The P-wave velocity V_P in the base rock, which may be assumed to be nearly isotropic, is 4.7 km/s, and the S-wave velocity is not measured. If the dynamic Poisson's ratio is assumed to be 0.2, the S-wave velocity may be estimated to be $V_S = 2.9$ km/s. If it is assumed that the elastic wave is transmitted without refraction, the distance from the AE source to the sensor will be given by $L = \frac{\Delta t \cdot V_P V_S}{V_P - V_S}$, using V_P, V_S and Δt, so that $L = 110$ m. Although the three-dimensional position cannot be determined from the arrangement of the sensor, it can be said that the AE source is at a

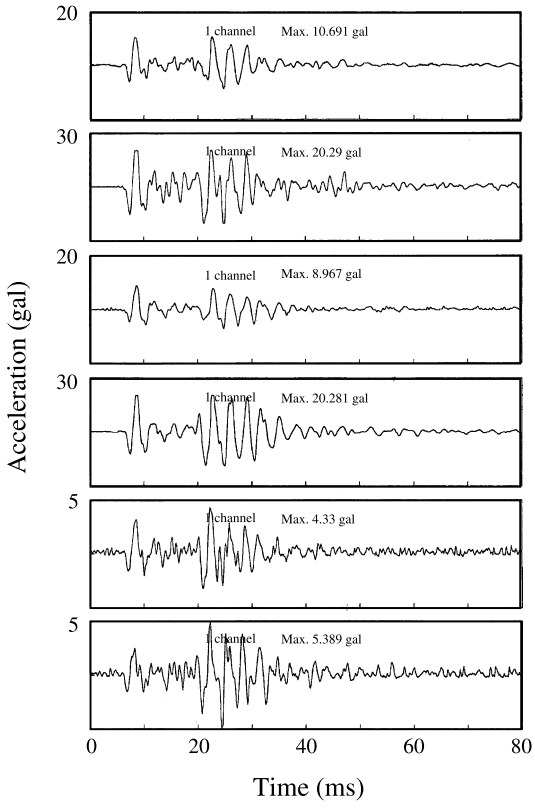

Fig. 14. Waveforms measured during one day of tunneling

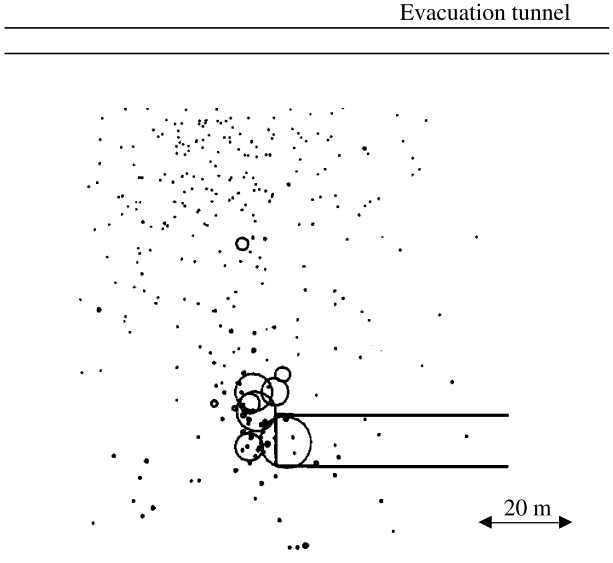

Fig. 15. AE sources concentrated near the face of the main tunnel after blasting

position near the face. Thus, many AE events with similar failure mechanisms occurred, each generating the same position in the measured waveform.

The epicenter of an AE event may be determined from the difference between the arrival times of the initial AE signals at the sensors placed in the evacuation tunnel. When the epicenters of these events were determined from the measurement data shown in Fig. 14, the plan view shown in Fig. 15 was obtained. Large-scale AE events are concentrated near the face. Because the distance between the face and the nearest sensor differs little from event to event, the influence of attenuation was disregarded, and for convenience the source energy of the AE events was set as the value obtained by multiplying the second power of the maximum amplitude by the duration.

Each circle represents a relative seismic energy. The actual area of fracture may have been considerably smaller than the area shown. All AE events were located as shown in Fig. 16. The major discontinuities in the figure are shown as short solid lines. It can be seen that the AE activities are situated along particular discontinuities. The accumulated energy of all AE events measured in the 150 m section from a point

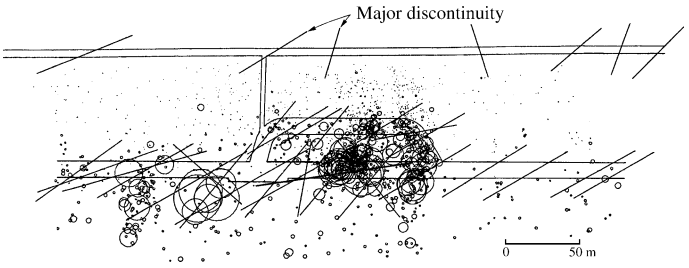

Fig. 16. AE sources determined in the noisy area, and major discontinuities

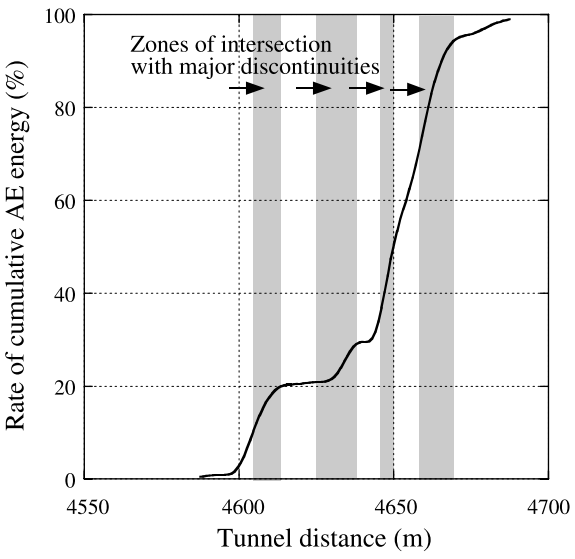

Fig. 17. Cumulative AE energy is shown to increase in zones of intersection with major discontinuities

4550 m into the tunnel is shown in Fig. 17. When the tunnel intersects with a major discontinuity, the AE energy increases.

3.3 Safety Management by AE Monitoring during Tunneling

Everyday safety control at the site was based on monitoring of AE events, calculation of the maximum amplitudes of AE measured, and observation around the rock face. Table 1 shows the criteria used to calculate risk, which were established by trial and error. Point A is calculated by multiplying the number of AE events by 1.6, and Point B is the maximum amplitude, which becomes ''saturated'' at 50 points when the measurement is 50 gal or more. Point C is allocated a value from 0 to 50, in accordance with the guidelines in Table 2, based on observations of rock noise and rock bursts at the working area. The type of support used is based on the total of Points A, B and C, as shown in Table 3.

The interpretation of this procedure, and its validity, require further examination. In a large-scale failure, the maximum amplitude becomes large, so if an AE event of large amplitude is observed, the possibility of large-scale instability is high. For this reason, the maximum AE amplitude is incorporated into the calculations of danger evaluation. Point C is allocated a value of 50 if a rock burst occurs at the face. In a

Table 1. Rating system for deciding the support type

	Item	Content
1.	Point A	Number of AE events × 1.6
2.	Point B	Maximum amplitude of AE (For amplitudes greater than 50 gal, value is 50 points)
3.	Point C	Observation of rock burst and rock noise (No rock noise: 0 point–rock burst: 50 points)

Total Point (T.P.) = Point A + Point B + Point C

Table 2. Ranking of state of tunnel face based on observation

Grade	State of tunnel face
I	No rock burst
II	Minimal rock noise
III	Substantial rock noise
IV	Very substantial rock noise
V	Rock burst

Table 3. Support types and scores evaluating danger of rock burst

Support class	T.P.
A (Normal support)	0–19
B = A + Shotcrete with steel fiber	20–49
C = B + Shotcrete on face	50–99
D = C + Rockbolt on face	>99

Normal support: Rockbolt and plain shotcrete on wall and arch
T.P. Total point

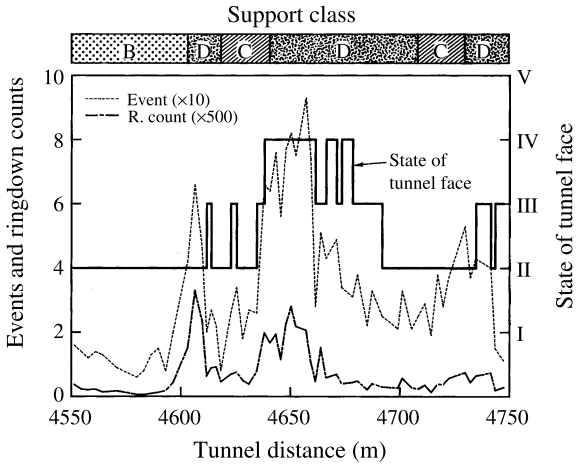

Fig. 18. Actual supports chosen, based on state of tunnel face, AE events and measured ring-down counts

case such as this, Point B is also likely to be given a value of 50. If a rock burst occurs near the face, even if it is about 100 m away, the acceleration is checked experimentally; if 50 or more gals are observed in this field, the risk evaluation will be given a value of 100 based on the values of Points B and C alone. If a rock burst suddenly occurs after minimal AE activity, it is possible to use heavy support. Conversely, even when Points B and C have low values, if AE activity is frequent, the danger of a rock burst is very high. In such a case, small-scale AE activity cannot be measured due to amplitude attenuation caused by wave transmission. For this reason, Point A is set as the number of AE events multiplied by 1.6.

Using this AE-based risk-management system, the excavation work was successfully executed, as shown in Fig. 18, which shows the relationship between AE measurements and the observed state of the face over a 200 m section of the excavation, and the actual supports adopted.

4. Conclusions

Rock bursts in tunnels are associated with the local stress field, the geological discontinuities, and the tunnel geometrical features, including direction and size. The possibility of a rock burst does not always depend on the magnitude of the overburden pressure. In the Kan-etsu tunnel, the tunnel face was found to be unstable when it approached particular discontinuities. Rock bursts and AE activities are mainly associated with a reduction of normal stress on discontinuities.

It is clear that rock bursts may occur even in areas of shallow overburden as long as certain conditions hold in the relationship between rock stress and discontinuities. If the deviation between the principal stresses is large, even in a location with a relatively small overburden, the danger is great.

To judge this quantitatively, three-dimensional measurement of rock stress is desirable. Under normal circumstances during tunnel construction, initial stress mea-

surement and stress analysis are hardly ever performed, and AE measurements are not used in everyday construction management. However, it may be possible to deduce the actual mechanism of a rock burst based on these measurements and analyses.

During construction of the final phase of the Kan-etsu tunnel, AE measurements were adopted empirically for selection of the type of support to be used and evaluation of hazards. These were found to be effective in everyday excavation management. Further work to be done in this area includes verification of the rationale behind the system.

References

Hirata, A., Taga, N., Kameoka, Y. (1991): AE monitoring and rock stress measurement in rock burst site. Proc. of 7th ISRM Congress (Aachen), 505–508.

Iwasaki, T., Kobayashi, R., Takata, A., Terada, M., Yamaguchi, U. (1972): Report on rock burst in metal mine. J. MMIJ Jpn. 1018, 901–906.

Minemoto, M. (1968): Rock burst in Shin-Shimizu tunnel. J. MMIJ Jpn. 965, 1216–1219.

Mitani, K., Aizawa, R., Yamamoto, T., Kameoka, Y. (1984): Tunnel excavation in rock burst area. In: Ken Mitani (ed.) Bull. Inst. Construction and Machine in Japan, 123–131.

Nakajima, I., Watanabe, Y. (1984): Acoustic emission monitoring of rock burst in excavation of the Kan-etsu tunnel. J. Progress AE Jpn. 2, 698–705.

Nakamichi, H. (1975): Plan of Kan-etsu tunnel under Tanigawa-dake mountain. J. Tunn. Undergr. Jpn. 6(1), 31–38.

Sugawara, K., Obara, Y., Okamura, H., Wang, Y., (1985): The determination of the complete state of stress in rock by the measurement of strains on a hemispherical borehole-bottom. J. MMIJ Jpn. 1167, 277–282.

Yamamoto, I., Taga, N. (1990): Second Kan-etsu tunnel project. J. Tunn. Undergr. Jpn. 21(2), 113–121.

Author's address: Atsuo Hirata, Sojo University, Ikeda 4-22-1, 860-0082 Kumamoto, Japan; e-mail: hirata@ce.sojo-u.ac.jp